(Received 6 November 2023, Accepted 26 December 2023, Scheduled 15 January 2024)

An Antipodal Vivaldi Antenna for a Drone-Mounted Ground Probing Radar

Stefano Pisa[1,*], Federico Pastori[1], Renato Cicchetti[1], Emanuele Piuzzi[1], Orlandino Testa[1], Erika Pittella[1], Andrea Cicchetti[2], Paolo d'Atanasio[3], and Alessandro Zambotti[3]

[1]*Department of Information Engineering, Electronics and Telecommunications, Sapienza University of Rome, Rome 00184, Italy*
[2]*Istituto Nazionale di Astrofisica, Via del Fosso del Cavaliere, 100, Rome 00133, Italy*
[3]*Italian National Agency for New Technologies, Energy and Sustainable Economic Development Casaccia Research Center, Rome 00123, Italy*

ABSTRACT: An antenna operating between 300 MHz and 700 MHz, designed to be used on a ground penetrating radar installed on an Unmanned Aerial Vehicle (UAV) for the exploration and characterization of the buried ice deposits on Mars, is presented. To this end, a lightweight, high-gain Vivaldi antenna having compact dimensions and high operating bandwidth has been taken into consideration. This antenna, equipped with circular-loaded rectangular slots etched on its radiating arms, exhibits improved performance in terms of size, return loss, gain, and fidelity factor with respect to a conventional antipodal Vivaldi antenna. Experimental measurements performed on a prototype of the Vivaldi antenna with slots showed a return loss lower than −12 dB with realized gains between 4 dBi and 6.5 dBi in the 300–700 MHz frequency band.

1. INTRODUCTION

The analysis and design of an antenna for a Ground Penetrating Radar (GPR) [1], useful to be installed on a drone, whose purpose will be the search for water ice in the first meters of depth of the Martian subsurface, is presented. Knowledge of the water ice location will enable on-site production of hydrogen and oxygen to power robotic missions or any future human exploration. The use of drones in the extremely rarefied atmosphere of Mars was demonstrated by the Mars helicopter, better known as Ingenuity, which operates on the planet Mars as part of the NASA mission "Mars 2020" [2]. In its first flight, performed on April 19, 2021, Ingenuity took off, reaching approximately 3 meters off the ground, completed a turn and then landed. Subsequently, the drone successfully performed further experimental flights covering ever greater distance and higher altitudes. To characterize the geometry and depth of the ice in the subsurface layers of the Martian crust, ESA has brought the Mars Express satellite into Mars orbit. This satellite was equipped with various instruments including the Mars Advanced Radar for Subsurface and Ionosphere Sounding (MARSIS) [3] a sub-surface sounding radar altimeter [4]. In the future developments of the ESA mission, the launch of another satellite equipped with a GPR installed on a drone is foreseen.To obtain a range resolution of at least 15 cm in the medium (assuming a basaltic soil with dielectric constant equal to 9), a radar pulse duration of about 3 ns, and therefore a band of about 400 MHz, is necessary. Furthermore, the Radar must be able to operate up to a depth of about 5 meters so, to reduce the attenuation through the mars ground and keep the dimensions of the antenna acceptable, a center frequency of about 500 MHz can be used. To this end, the GPR should be equipped with a light and compact antenna suitable to operate between 300 MHz and 700 MHz. To meet these requirements, planar printed antennas such as Vivaldi, log-periodic, sinuous and bow-tie antennas appear to be good candidates.

As well known, Vivaldi antennas can be either coplanar or antipodal [5, 6]. Two metallic arms, having exponential profile, are printed over a dielectric substrate in the so called coplanar configuration. The feeding circuit, made with a microstrip loaded with a quarter wave radial stub located on the bottom side of the substrate, crosses the antenna radiating arms. To simplify the feeding circuit, the so-called antipodal Vivaldi antenna was developed. It provides the printing of the radiating arms on both faces of a dielectric substrate, thus allowing a direct connection of both arms to a simple connector. The Vivaldi antenna was first proposed by Gibson to be integrated into a video receiver operating between 8 GHz and 40 GHz [5]. An antipodal Vivaldi antenna with resistive layer was presented in [6]. The antenna operates over the frequency band from 3.1 GHz to 10.6 GHz with a gain between 4 dBi and 11 dBi in the specified band. Although the Vivaldi antenna was initially conceived for applications in the microwave band, a realization in the UHF band with a reflection coefficient lower than −6 dB from 125 MHz up to 900 MHz and a gain greater than 3 dB above 320 MHz, was suggested in [7]. This antenna was realized on a flexible silicone foam substrate with dimensions 600 × 600 mm^2. A Vivaldi antenna, having dimensions 530 × 793 mm^2 and a reflection coefficient lower than −10 dB in the frequency band between 253 MHz and 513 MHz with a maximum gain of 6.6 dBi at 469 MHz, was used as a sensor

* Corresponding author: Stefano Pisa (stefano.pisa@uniroma1.it).

for a GPR in [8]. An antipodal Vivaldi antenna for detecting UHF signals radiated by electrical discharges in high voltage transformers was proposed in [9]. To improve the performances of the antenna, some slits were engraved on its radiating arms. These slots focus the surface currents on the inner edge of the radiating arms with a consequent increase in the radiated energy and gain, particularly in the lower end of frequency band where an improvement in antenna matching impedance is also obtained. Doing so, the realized antenna exhibits a frequency band between 0.8 GHz and 3 GHz with a gain of -3 dBi at 1 GHz and 9 dBi at 3 GHz [9]. A Vivaldi antenna, for an aircraft mounted GPR system for detecting buried mines, was described in [10]. To extend the antenna impedance band towards low frequencies, without changing the antenna size ($220 \times 220\,\text{mm}^2$), a set of non-symmetrical rectangular corrugations was realized on the non-radiating side of the antenna. In this way, a reflection coefficient less than -7 dB in the frequency band between 600 MHz and 3000 MHz and a gain increasing with the frequency between 6 dBi and 12 dBi was achieved.

Printed log-periodic antennas consist of a series of dipoles, all fed and aligned along an axis orthogonal to the feeding line, whose lengths vary according to the logarithm of the working frequency. Each dipole resonates at the frequency at which its length is approximately equal to half the wavelength. In resonance condition, dipoles of greater length act as reflectors while dipoles of shorter length act as directors. The overall frequency response of the antenna is sufficiently flat when the tails of the radiated fields from the various elementary radiators constructively add up in the desired frequency band.These antennas are usually made with metal dipoles in air or printed on a planar dielectric substrate. In the latter case, a compact, light, robust and low-cost antenna is obtained. Carrel, in 1961, introduced a mathematical model for the analysis of LPDA, the results of which agreed reasonably well with the experimental values [11]. A PLPDA with 12 dipoles suitable to operate in a frequency band between 0.8 GHz and 2.5 GHz was designed in [12]. The realized antenna presented a reflection coefficient lower than -12 dB and a gain ranging between 4.5 dBi and 6.3 dBi in the band of interest. A log-periodic antenna with 10 dipoles operating between 0.8 GHz and 6 GHz was proposed in [13]. Unlike the usual LPDAs, in this antenna the feeding connector has been connected near the shortest dipole obtaining a reflection coefficient always lower than -10 dB and a gain of about 4 dBi in the considered band. To reduce the antenna dimensions, widening the working band, all the dipoles were shaped like a bow-tie [14, 15], while only the longest dipole was replaced with a triangular shaped dipole in [16]. In any case, due to the different resonant processes taking place in the different dipoles that make up a log-periodic antenna, the ringing level is not compatible with time-domain pulsed applications.

The sinuous antenna, first proposed in a patent by DuHamel in 1987 [17], has four arms, each shifted 90° away from each other appearing as a combination of a spiral and a logarithmic antenna. This geometry enables sinuous antennas to have wide impedance bandwidth with polarization diversity. Moreover, since any pair of antenna arms that are opposite to each other are excited via a balun, it is possible to excite a field with left circular polarization (LHCP) or right circular polarization (RHCP), respectively. As the log-periodic antennas, sinuous antennas suffer from resonances that produce late time ringing which is particularly problematic for sensing applications. To remove this drawback, a novel truncation method suitable to avoid the sharp end resonance was presented in [18], while some technical solutions aimed to ensure the optimal trade-off between antenna size and radiation behavior were presented in [19]. To this end, modifications of the antenna geometry based on the meandering as well as on the loading with dielectric structures were proposed. Only a few works have reported sinuous antennas operating in the UHF band. In [20], the design of a compact dually polarized antenna, working in the 500 MHz–3000 MHz frequency range, was proposed. The antenna diameter was 250 mm, and a ground plane of dimension 250 mm $\times$ 250 mm, 30 mm behind the slot antenna was employed to achieve a directive radiation pattern. The antenna proposed in [21] had an impedance bandwidth in the range of 0.45 GHz–6 GHz with a reference impedance of 100 ohms and a diameter of about 290 m. The performance of the fabricated antenna with wideband balun was verified evidencing a gain between -1 dBi and 5.5 dBi.

A bow-tie antenna consists of two triangular arms etched on a planar substrate and fed at the arms' apex. The first comprehensive investigation of the input impedance and radiative performances from bow-tie antennas was performed by Brown and Woodward in 1952 [22]. Their investigations showed that unipolar bow-ties are more broadband than cylindrical monopoles, though they are less broadband than corresponding conical monopoles. To minimize the late ringing time of the antenna, caused by surface current reflections, resistive loading has been suggested in [23, 24]. In particular, the antenna presented in [24] was based on a wire bow-tie structure with resistors of different values placed on the radiating elements. In [25], size reduction was achieved by using a dual-layer bow-tie with a folded structure and meandered microstrip lines on the backside of the antenna. In the reported applications bow-tie antennas were employed for underground monitoring and for medical diagnostics and optimized to operate in contact with a dielectric medium. To enhance the free-space radiation characteristics of the bowtie antenna, a cavity-backed structure was utilized [26]. The antenna prototype was matched in the 2 GHz–5.5 GHz band with a gain ranging between 8 dBi and 10 dBi. A -10 dB impedance bandwidth of 97.9% with a broadside gain of at least 2 dBi was obtained inserting radially aligned grooves in the radiators' ends [27].

In order to mitigate the back radiation level and to ensure unidirectional far-field radiation patterns both sinuous and bow-tie antennas are equipped with absorbing cavities which reduces antenna efficiency and bandwidth. Furthermore, both antennas have a beam-former circuitry necessary for the proper current arms phasing, making the manufacture of these antennas rather complex and expensive. Concerning log periodic antennas, they are made up of a cascade of resonant elements and therefore have high ringing and low gains.

Based on the considerations discussed above, a Vivaldi geometry was chosen to be used in the 300 MHz–700 MHz band in a drone land survey radar. In particular, an antipodal Vivaldi

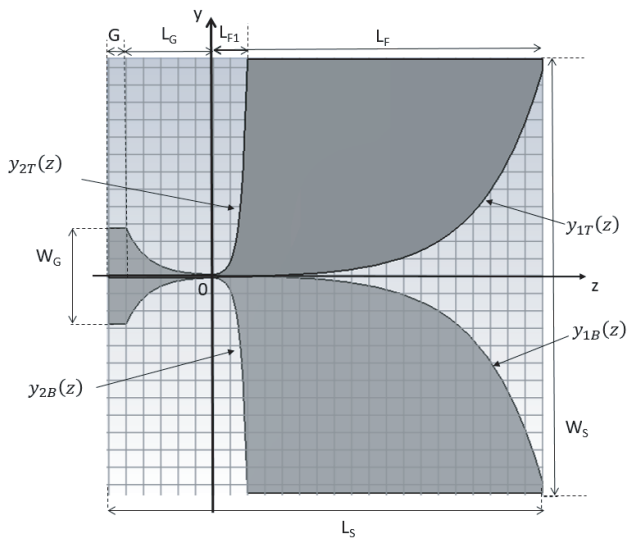

FIGURE 1. Geometry of the standard antipodal Vivaldi antenna.

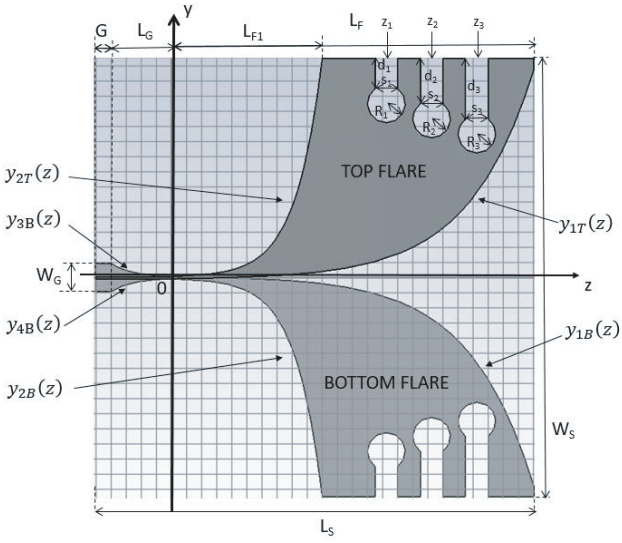

FIGURE 2. Geometry of the antipodal Vivaldi antenna with circularly-loaded rectangular slots.

antenna, equipped with suitable rectangular slots loaded with circular terminations in order to improve its gain, return loss and to reduce its overall dimensions, is presented in this paper.

2. ANTENNA DESIGN METHODOLOGIES

2.1. Standard Antipodal Vivaldi Antenna

Figure 1 shows the geometry of a standard antipodal Vivaldi antenna.

The exponential profile curves in the region between 0 and LF can be described by the following equations [7]:

$$y_{1T}(z) = A_T + e^{mz} \qquad 0 < z < LF \tag{1}$$

$$y_{2T}(z) = B_T + e^{nz} \qquad 0 < z < \left(\frac{1}{n}\right)\ln\left(\frac{W_S}{2} - B_T\right) \tag{2}$$

$$y_{1B}(z) = -(A_B + e^{mz}) \qquad 0 < z < LF \tag{3}$$

$$y_{2B}(z) = -(B_B + e^{nz}) \qquad 0 < z < \left(\frac{1}{n}\right)\ln\left(\frac{W_S}{2} - B_B\right) \tag{4}$$

where m and n are parameters defining the growth of the curve, while A and B are constants representing the value of $y(z)$ at $z = 0$.

Once W_S, L_F, and L_{F1} have been identified, the equations defining the parameters m and n can be computed as:

$$m = \frac{1}{L_F} \cdot \ln\left(\frac{W_S}{2} - A_T\right) \tag{5}$$

$$n = \frac{1}{L_{F1}} \cdot \ln\left(\frac{W_S}{2} - B_T\right) \tag{6}$$

The exponential profile curves, in the spatial region between $-L_G$ and 0, employed to improve the antenna impedance matching are described by the following equations:

$$y_{3B}(z) = -A_B - 2 + e^{nz} \qquad -LG < z < 0 \tag{7}$$

$$y_{4B}(z) = -B_B - e^{nz} \qquad -LG < z < 0 \tag{8}$$

Finally, a rectangular ground plane of length G and width W_G is added near the connector location (see Fig. 1). The width of the feeding microstrip w_m useful to realize a $50\,\Omega$ microstrip line can be obtained using the equations reported in [28].

2.2. Vivaldi Antipodal Antenna with Circularly-Loaded Rectangular Slots

To improve the performance of the Vivaldi antenna, circularly-loaded rectangular slots can be etched on the antenna arms [9, 29]. As shown in Fig. 2, the etches are characterized by their width (s), length (d), radius of the circular termination (R), and position (z). The remaining parts of the structure are the same as the standard antipodal Vivaldi antenna described above.

2.3. Fidelity Factor

An important characteristic of a UWB antenna is the fidelity factor defined as the peak value of the cross-correlation function between the observed pulse $s2(t)$ (electric field) at a given distance from the antenna and the antenna exciting pulse $s1(t)$ (input voltage):

$$F = \frac{\int_{-\infty}^{+\infty} s1(t) \cdot s2(t+\tau)dt}{\sqrt{\int_{-\infty}^{+\infty} s1^2(t)dt}\sqrt{\int_{-\infty}^{+\infty} s2^2(t)dt}} \tag{9}$$

where τ is the time delay maximizing F [30].

3. RESULTS AND DISCUSSION

All the considered antennas were designed using an FR4 substrate ($\varepsilon_r = 4.4$, $\tan\delta = 0.015$) with thickness $H = 1.6$ mm. The electromagnetic performances of all the considered anten-

$A_T = A_B$	-2.45 mm		$B_T = B_B$	0.45 mm
m	0.01157		n	0.028912
L_F	495 mm		L_{F1}	200 mm
L_G	91.37 mm		G	29.24 mm
W_S	650 mm		L_S	615.6 mm

Table 1. Parameters of the standard antipodal Vivaldi antenna.

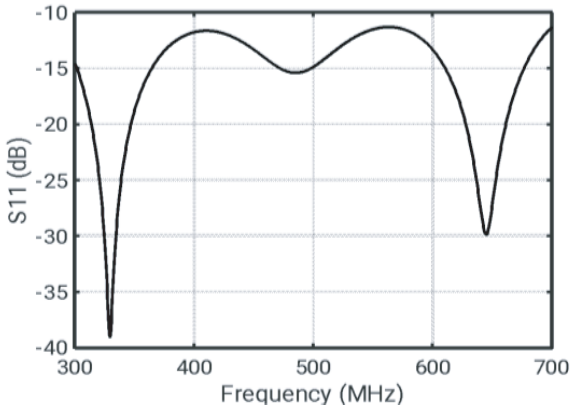

FIGURE 3. Magnitude of the computed reflection coefficient of the Vivaldi antenna.

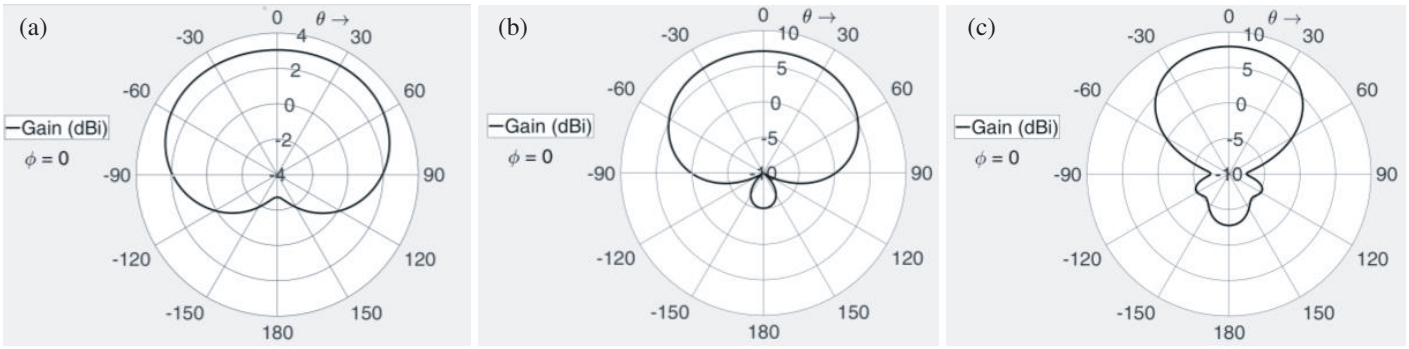

FIGURE 4. Radiation patterns of the standard Vivaldi antenna at (a) 300 MHz, (b) 500 MHz and (c) 700 MHz.

nas were evaluated using the CST Studio Suite full-wave software.

3.1. Design of the Vivaldi Antipodal Standard Antenna

The first designed antenna is the antipodal Vivaldi antenna. Following the indications given in [6], $W = L_F = \frac{c}{f_{\min}}\sqrt{\frac{2}{\varepsilon_r+1}} = 600$ mm was set. Parameters A_B, A_T, B_B, and B_T in Eqs. (1)–(8) have been defined in order to have a feeding line characteristic impedance equal to 50 Ω. For the considered substrate $w_m = 2.86$ mm is required [28] that has been achieved by choosing $A_T = A_B = -2.45$ mm and $B_T = B_B = 0.45$ mm. Furthermore, $L_{F1} = 200$ mm, $L_G = 80$ mm and $G = 20$ mm were set. The geometric antenna parameters L_{F1}, L_G, G, m and n have been optimized using the Trust Region Framework optimizer available in CST Microwave Studio. In particular, to take into account variations caused by material and manufacturing tolerances, the threshold of the parameter $|S_{11}|_{\text{dB}}$ was chosen equal to -13 dB in the band of interest. After optimization the values reported in Table 1 have been obtained.

The excitation signal employed to evaluate the antenna fidelity factor is a Gaussian modulated sinusoid:

$$s_1(t) = e^{\frac{-(t-t_0)^2}{2\sigma^2}}\cos(2\pi f_0 t) \tag{10}$$

where: $f_0 = \frac{f_{\text{MAX}}+f_{\text{MIN}}}{2}$, $B = f_{\text{MAX}} - f_{\text{MIN}}$, $\sigma = \frac{1}{\sqrt{2}B}$, $t_0 = \frac{5}{\sqrt{2}B}$, $f_{\text{MIN}} = 300$ MHz, and $f_{\text{MAX}} = 700$ MHz. The signal $s_2(t)$ was evaluated in the antenna far field at a 2 m distance from the antenna center. A fidelity factor equal to $F = 0.9852$ was computed for this antenna.

A computed reflection coefficient lower than -10.5 dB in the 300 MHz–700 MHz frequency band is observed in Fig. 3. The -13 dB goal is not reached by the optimizer, but in any case a good matching is obtained in the whole frequency band. Fig. 4 shows the antenna radiation patterns at (a) 300 MHz, (b) 500 MHz, and (c) 700 MHz. From these figures it appears that the antenna exhibits a realized gain of 2.74 dBi, 6.63 dBi, and 7.13 dBi at 300 MHz, 500 MHz and 700 MHz, respectively.

3.2. Design of a Vivaldi Antipodal Antenna with Circular-Ended Rectangular Slots

To improve the performance of the standard Vivaldi antenna three circular-ended rectangular slots have been added to the top and bottom radiating arms (see Fig. 2). The optimization of the antenna parameters was performed with the Trust Region Framework optimizer of CST so to guarantee a $|S_{11}|_{dB} < -13$ dB. The parameters obtained after the optimization are reported in Table 2.

$A_T = A_B$	-2.45 mm		$B_T = B_B$	0.45 mm
m	1.1711		n	0.02834
L_F	480 mm		L_{F1}	200 mm
L_G	80 mm		G	20 mm
z_1	285 mm		d_1	60 mm
z_2	345 mm		d_2	80 mm
z_3	405 mm		d_3	100 mm
s_1	30 mm		R_1	10 mm
s_2	30 mm		R_2	10 mm
s_3	30 mm		R_3	10 mm
W_S	580 mm		L_S	580 mm

Table 2. Parameters of the Vivaldi antipodal antenna with circular ended rectangular slots.

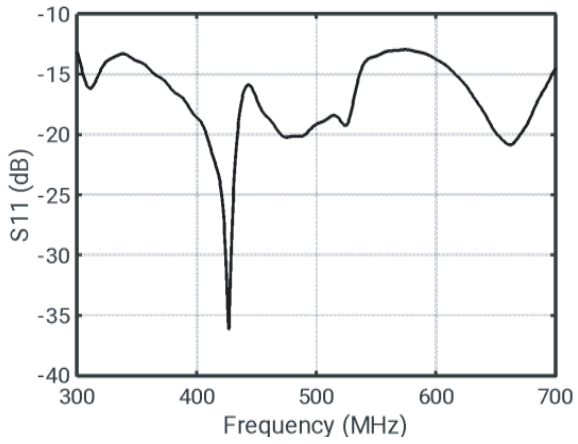

FIGURE 5. Reflection coefficient of the slotted Vivaldi antenna simulated with the CST.

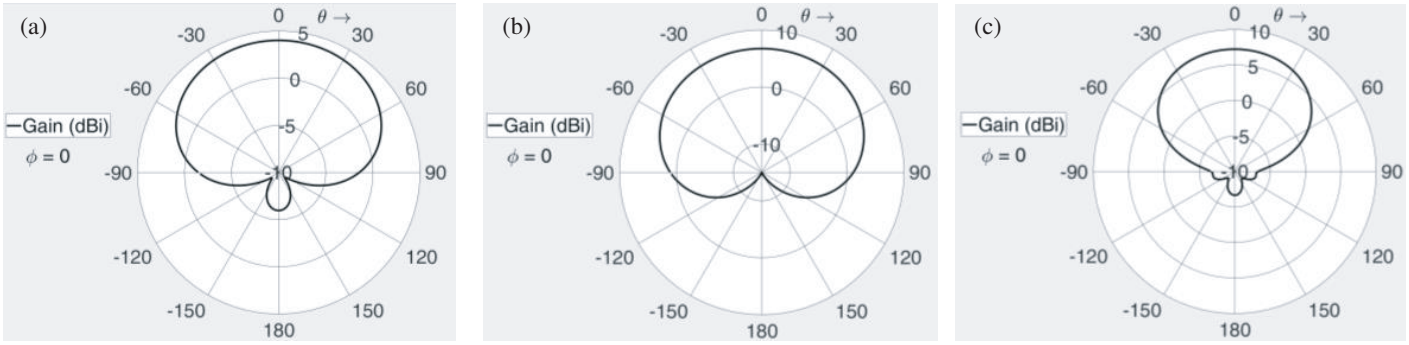

FIGURE 6. Radiation patterns of the slotted Vivaldi antenna at (a) 300 MHz, (b) 500 MHz and (c) 700 MHz.

The frequency behavior of the computed antenna reflection coefficient is shown in Fig. 5, while the radiation diagrams at the frequencies of 300 MHz, 500 MHz, and 700 MHz are reported in Fig. 6. As can be observed, the reflection coefficient is below -13 dB, while the antenna realized gain assumes values of 4.18 dBi, 6.96 dBi, and 7.59 dBi at 300 MHz, 500 MHz and 700 MHz, respectively. Finally, a fidelity factor $F = 0.9874$ has been computed.

Comparing the performance of the two considered antennas, it can be noticed that the Vivaldi antenna equipped with circular-ended rectangular slots is more compact (its size being 580 mm $\times$ 580 mm with respect to the 650 mm $\times$ 615.6 mm of the standard Vivaldi), and it has a reflection coefficient lower than -13 dB (compared to -10.5 dB of the standard Vivaldi), and a higher realized gain and fidelity factor.

Figure 7 shows the surface current magnitude distribution of both (a) standard and (b) slotted antennas excited at the frequency of 300 MHz. Comparing the figure, it can be observed that the slots are able to reduce the unwanted surface currents that radiate energy along the lateral arms (region A), focusing the current distribution along the antenna radiating inner edge (region B) thus increasing the effective current path length, thereby improving the antenna gain and the return loss.

4. ANTENNA REALIZATION AND MEASUREMENTS

A prototype of the Vivaldi antenna with circular-ended rectangular slots has been realized on a cheap FR4 substrate [see Fig. 8(a)] with a total weight of 1025 gr. Obviously, substrates qualified for space applications, like those from the Rogers company [31], having electrical characteristics and thicknesses similar to those of FR4 can be chosen for the final antenna realization.

The return loss of the antenna always remains lower than -12 dB in the 300 MHz 700 MHz frequency band, as can be seen from the experimental measurements carried out with the Agilent E8363C network analyzer (see Fig. 8(b)). Furthermore, a good agreement with the numerical simulations performed with the CST full-wave software can be observed.

The radiation pattern measurements were performed in a semi-anechoic chamber available at the ENEA-Casaccia Center (see Fig. 9). The chamber is equipped with a log periodic ELECTROMETRICS LPA25/30 transmitting antenna fed by an Agilent 8648D RF generator, while the antenna under test is connected to an Agilent E4440A spectrum analyzer. The radiation patterns computed and measured at 300 MHz, 500 MHz and 700 MHz, respectively are reported in Fig. 10. A good

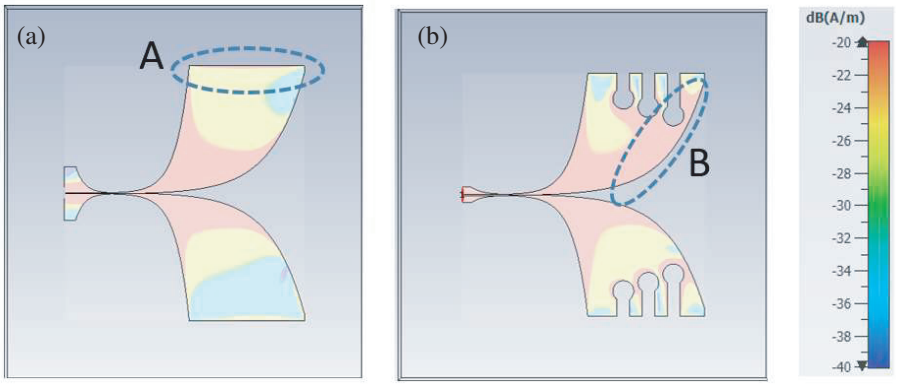

FIGURE 7. Surface current magnitude distribution of the (a) standard and (b) slotted Vivaldi antenna at 300 MHz. The increase of the surface current density along the radiating slot of the Vivaldi antenna equipped with the circular-ended rectangular slots is evident in the figure.

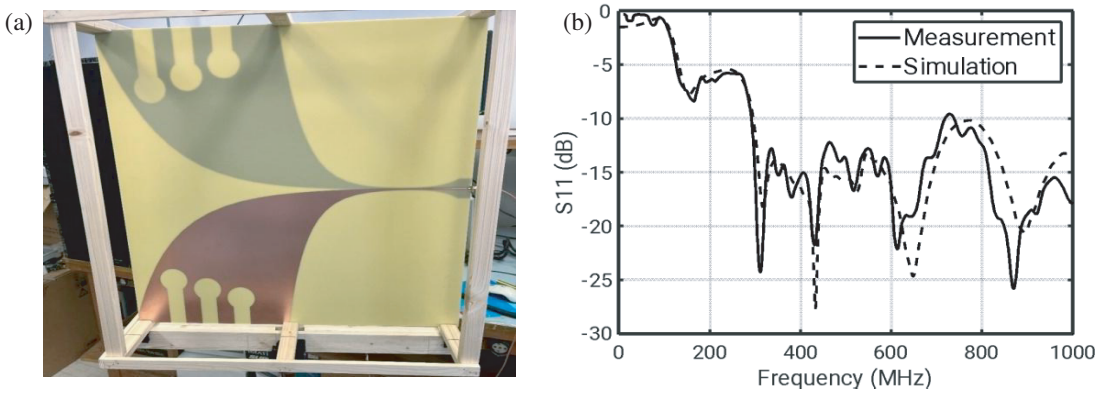

FIGURE 8. (a) Picture of the manufactured antenna. (b) Frequency behavior of the input reflection coefficient of the slotted Vivaldi antenna.

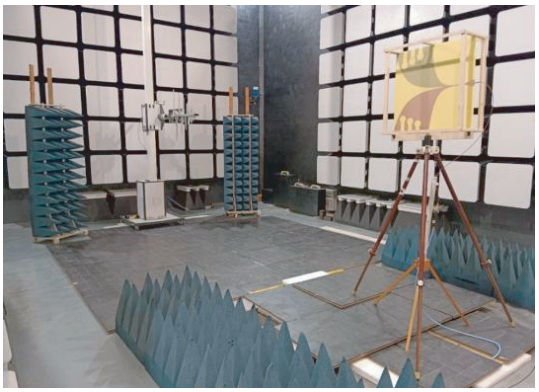

FIGURE 9. Antenna setup in the anechoic chamber.

agreement between measurements and simulations is observed.

The gain measurement, performed by substitution using the SEIBERSDORF PCD-8250 antenna as a reference, is reported in Fig. 11. The measured antenna gain varies from 4 dBi to 6.2 dBi within the antenna operating band. The small difference observed between measurements and numerical simulations are probably related to the manufacturing tolerances.

A comparison in terms of bandwidth, size, return loss, and gain between the proposed antenna and those already available in the literature is reported in Table 3. To the authors' knowledge, no antennas with the required bandwidth have been yet presented in literature. The only comparable antenna is the one proposed in [7]. As can be seen from the table, the antenna in [7] has dimensions similar to those of the Vivaldi antenna proposed in this work with a higher fractional bandwidth but with a worse return loss.

4.1. Slot Vivaldi Antenna Time Domain Measurements

The time domain antenna performance has been investigated to evaluate its suitability in the Radar analysis of layered structures. When the antenna is used for distance measurements it is necessary to estimate the time delay (τ_D) between the VNA calibrated ports and the antenna aperture plane. This delay can be evaluated simply by placing a transmitting and receiving antenna, connected to the VNA, facing each other. To this end, the Agilent E8363C network analyzer was used to synthesize by the time domain reflection (TDR) a pulse with an initial frequency of 300 MHz and a stop frequency of 700 MHz. The time behavior of the pulse generated by the analyzer and of its envelope are reported in Fig. 12.

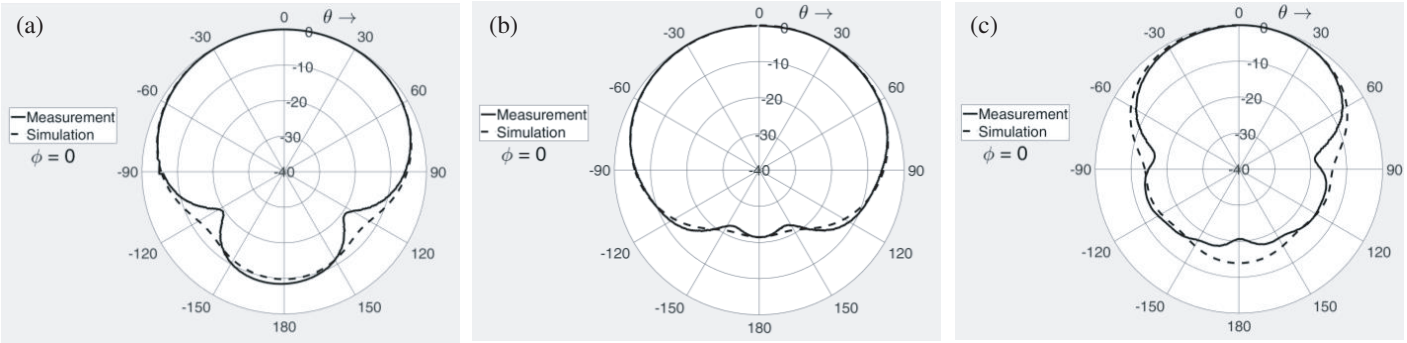

FIGURE 10. Radiation patterns of the slotted Vivaldi antenna at (a) 300, (b) 500 and (c) 700 MHz. A good agreement between computed and measurements results is observed.

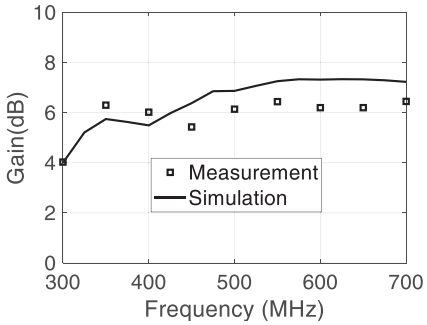

FIGURE 11. Gain of the slotted Vivaldi antenna as a function of the frequency. A good agreement between numerical simulation and experimental measurement performed on antenna prototype is observed.

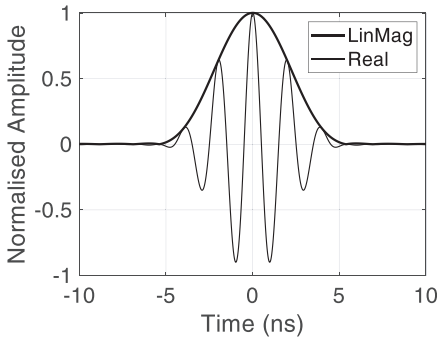

FIGURE 12. Pulsed-signal generated by the PNA.

TABLE 3. Comparison between the proposed antenna and those already available in the literature.

Ref.	Bandwidth [MHz]	Fractional Bandwidth %	Dimensions Width × Length [mm^2]	Retur Loss [dB]	Gain Min-Max [dBi]
[7]	150–900	140	600 × 600	> 6	1–7.6
[8]	253–513	68	530 × 793.3	> 10	0–6.6
[10]	500–3000	143	220 × 220	> 7	6–12
[32]	500–2000	120	260 × 185	> 10	2–7
This work	300–700	80	580 × 580	> 12	4.18–7.59

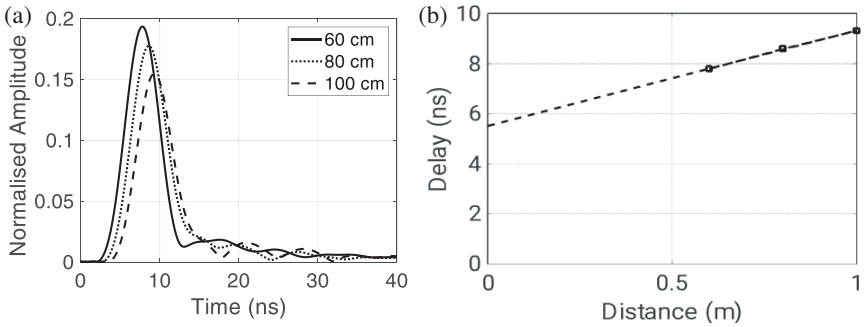

FIGURE 13. (a) Envelope pulse response for various antenna distances and (b) delay-distance plot.

By analyzing the time domain pulse response on the VNA, it is possible to determine the signal delay time between the two calibrated ports. This measurement must be repeated for different distances and finally, through a linear regression formula, the intercept point of the resulting fitting line with the delay axis is the searched delay time τ_D. Having realized two samples of

the same antenna the above described measurements were performed by linking the two antennas to the two calibrated ports of the PNA, placing them facing each other and measuring the $S_{21}(t)$ scattering parameter.

The measured responses are reported in Fig. 13(a), while Fig. 13(b) shows the delay-distance plot for the two antennas from which a delay value $\tau_D = 5.52/2 = 2.76$ ns has been extrapolated for each antenna corresponding to an antenna electrical length in free space equal to: $L_E = c * \tau_D = 0.83$ m, where c is the speed of light in free-space.

Further measurements have been performed by placing the antenna in front of a metallic panel and measuring the $S_{11}(t)$ scattering parameter for various antenna panel distances. The responses for distances equal to 120 cm and 135 cm are reported in Fig. 14.

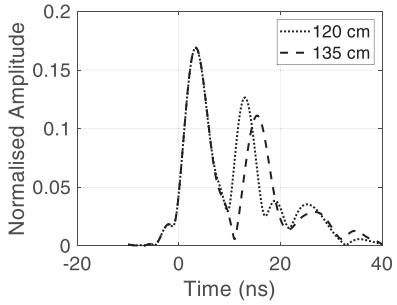

FIGURE 14. Envelope pulse response for 120 cm and 135 cm antenna-panel distances.

In this case, the first peak at 3.3 ns is due to the antenna reflections while the peaks at 13 ns and 15 ns are due to the panel. By taking into account the antenna delay, the peaks correspond to a distance of 112 and 142 cm with errors of 8 cm and 7 cm, respectively. Hence, the radar system equipped with the proposed antenna is able to evaluate a targets distance in free space with errors lower than 10 cm.

5. CONCLUSION

An antipodal Vivaldi antenna useful to be employed in space drones, aimed at analyzing traces of water in the Martian subsurface, has been presented. The antenna, having a central frequency of 500 MHz and a bandwidth of 400 MHz, can operate with impulsive signals suitable for carrying out a survey of the Martian surface up to about 5 m depth. A prototype of the proposed antenna exhibits a return loss better than -12 dB in the 300 MHz–700 MHz band with a realized gain between 4 dBi and 6.5 dBi. Furthermore, sizes and weight were found lower than those of similar antennas already available in the literature.

REFERENCES

[1] Daniels, D. J., *Ground Penetrating Radar*, IET, 2004.

[2] "Mars Helicopter — NASA's Mars Exploration Program," Available on line at: https://mars.nasa.gov/technology/helicopter/#Overview.

[3] Picardi, G., J. J. Plaut, D. Biccari, O. Bombaci, D. Calabrese, M. Cartacci, A. Cicchetti, S. M. Clifford, P. Edenhofer, W. M. Farrell, and e. al., "Radar soundings of the subsurface of Mars," *Science*, Vol. 310, No. 5756, 1925–1928, 2005.

[4] "Mars Express — European Space Agency Mission," Available on line at: https://www.esa.int/Science_Exploration/Space_Science/Mars_Express_overview.

[5] Gibson, P. J., "The vivaldi aerial," in *1979 9th European Microwave Conference*, 101–105, 1979.

[6] Abbosh, A. M., "Directive antenna for ultrawideband medical imaging systems," *International Journal of Antennas and Propagation*, Vol. 2008, 854012, 2008.

[7] Presse, A., J. M. Floc'h, A.-C. Tarot, and C. Camus, "Broadband uhf flexible vivaldi antenna," in *2013 Loughborough Antennas & Propagation Conference (LAPC)*, 277–280, 2013.

[8] Guerra-Huaranga, T., R. Rubio-Noriega, and M. Clemente-Arenas, "Comparative analysis of three types of vhf/uhfantennas for gpr array," in *2020 IEEE MTT-S Latin America Microwave Conference (LAMC 2020)*, 1–4, 2021.

[9] Zhang, J., X. Zhang, and S. Xiao, "Antipodal vivaldi antenna to detect uhf signals that leaked out of the joint of a transformer," *International Journal of Antennas and Propagation*, Vol. 2017, 9627649, 2017.

[10] García Fernández, M., G. □. Narciandi, A. Arboleya, C. V. Antuña, F. L.-H. Andrés, and Y. □. López, "Development of an airborne-based gpr system for landmine and ied detection: Antenna analysis and intercomparison," *IEEE Access*, Vol. 9, 127 382–127 396, 2021.

[11] Carrel, R. L., "Analysis and design of the log-periodic dipole antenna," *Technical Report No. 52*, Elec. Univ. of Illinois, 1961.

[12] Mistry, K. K., P. I. Lazaridis, Z. D. Zaharis, T. D. Xenos, E. N. Tziris, and I. A. Glover, "An optimal design of printed log-periodic antenna for l-band emc applications," in *2018 IEEE International Symposium on Electromagnetic Compatibility and 2018 IEEE Asia-Pacific Symposium on Electromagnetic Compatibility (emc/apemc)*, 1150–1155, 2018.

[13] Chopade, P. and S. V. Gaikwad, "Design and analysis of log periodic dipole array antenna," *Ictact. J. Microelectron.*, Vol. 5, 836–844, 2019.

[14] Abdulhameed, A. A. and Z. Kubik, "Design a compact printed log-periodic biconical dipole array antenna for emc measurements," *Electronics*, Vol. 11, No. 18, 2877, Sep. 2022.

[15] Pisa, S., S. Chicarella, E. Pittella, E. Piuzzi, O. Testa, and R. Cicchetti, "A double-sideband continuous-wave radar sensor for carotid wall movement detection," *IEEE Sensors Journal*, Vol. 18, No. 19, 8162–8171, Oct. 2018.

[16] Mistry, K. K., I. Lazaridis, Z. D. Zaharis, and T. H. Loh, "Design and optimization of compact printed log-periodic dipole array antennas with extended low-frequency response," *Electronics*, Vol. 10, No. 17, 2044, Sep. 2021.

[17] Duhamel, R. H., "Dual polarized sinuous antennas," US Patent 4,658,262, 1987.

[18] Crocker, D. A. and J. Scott, "On the design of sinuous antennas for uwb radar applications," *IEEE Antennas and Wireless Propagation Letters*, Vol. 18, No. 7, 1347–1351,

Jul. 2019.

[19] Mescia, L., G. Mevoli, C. M. Lamacchia, M. Gallo, P. Bia, D. Gaetano, and A. Manna, "Sinuous antenna for uwb radar applications," *Sensors*, Vol. 22, No. 1, Jan. 2022.

[20] Bellion, A., C. L. Meins, A. Julien-Vergonjanne, and T. Monediere, "A new compact dually polarized direction finding antenna on the uhf band," in *2008 IEEE Antennas and Propagation Society International Symposium*, Vol. 1-9, San Diego, Ca, Jul. 2008.

[21] Kim, D., C. Y. Park, Y. Kim, H. Kim, and Y. J. Yoon, "Four-arm sinuous antenna with low input impedance for wide gain bandwidth," *IEEE Access*, Vol. 10, 35 265–35 272, 2022.

[22] Brown, G. H. and O. M. Woodward, "Experimentally determined radiation characteristics of conical and triangular antennas," *RCA Review*, Vol. 13, No. 4, 425–452, 1952.

[23] Lestari, A., A. G. Yarovoy, and L. P. Ligthart, "An efficient ultra-wideband bow-tie antenna," in *2001 31st European Microwave Conference*, 1–4, 2001.

[24] See, C. H., R. A. Abd-Alhameed, S. W. J. Chung, D. Zhou, H. Al-Ahmad, and P. S. Excell, "The design of a resistively loaded bowtie antenna for applications in breast cancer detection systems," *IEEE Transactions on Antennas and Propagation*, Vol. 60, No. 5, 2526–2530, May 2012.

[25] Li, X., M. Jalilvand, Y. L. Sit, and T. Zwick, "A compact double-layer on-body matched bowtie antenna for medical diagnosis," *IEEE Transactions on Antennas and Propagation*, Vol. 62, No. 4, 1808–1816, Apr. 2014.

[26] Qu, S.-W., J.-L. Li, Q. Xue, and C. H. Chan, "Wideband cavity-backed bowtie antenna with pattern improvement," *IEEE Transactions on Antennas and Propagation*, Vol. 56, No. 12, 3850–3854, Dec. 2008.

[27] De Mello Goncalves Licursi, R., A. C. Lepage, and X. Begaud, "The bow-tie antenna: Performance limitations and improvements," *IET Microwaves Antennas & Propagation*, Vol. 16, No. 5, 283–294, Apr. 2022.

[28] Pozar, D. M., *Microwave Engineering*, John Wiley & Sons, 2011.

[29] Tahar, Z., X. D. Benslama, and M., "An ultra-wideband modified vivaldi antenna applied to through the ground and wall imaging," *Progress In Electromagnetics Research C*, Vol. 86, 111–122, 2018.

[30] Lamensdorf, D. and L. Susman, "Baseband-pulse-antenna techniques," *IEEE Antennas and Propagation Magazine*, Vol. 36, No. 1, 20–30, 1994.

[31] Rogers Corporation, A. Z. C., "Low outgassing characteristics of rogers laminates approved for spacecraft applications," USA, 2002.

[32] Fioranelli, F., S. Salous, I. Ndip, and X. Raimundo, "Through-the-wall detection with gated fmcw signals using optimized patch-like and vivaldi antennas," *IEEE Transactions on Antennas and Propagation*, Vol. 63, No. 3, 1106–1117, 2015.